Automatic Detection and Tracking of Infrared Aerial Targets via Singular Value Decomposition in the Event of Infrared Jamming

Bader Algahtani, Prof. Adnan Affandi

Department of Electrical and Computer Engineering
King Abdulaziz University, Jeddah, Saudi Arabia

DOI: 10.29322/IJSRP.13.09.2023.p14111
https://dx.doi.org/10.29322/IJSRP.13.09.2023.p14111

Paper Received Date: 17th July 2023
Paper Acceptance Date: 26th August 2023
Paper Publication Date: 6th September 2023

Abstract – Detecting and tracking an infrared (IR) aerial target in the event of infrared jamming is still challenging. In this paper, singular value decomposition (SVD) based algorithms are proposed for the detection and tracking of aerial targets in the presence of decoy flares. Features including brightness intensity, dominant orientation and complexity were used for the discrimination against decoy flares. SVD characteristics including oriented energy analysis, image energy truncation, and low rank approximation were used to measure these features. Obtained results show that brightness based discrimination has a better performance against decoy flares compared to orientation based and complexity based discrimination. In addition, orientation based algorthim was able to discriminate between aerial targets like helicopters and decoy flares via the dimensions of aerial target parts such as rotor blade surfaces.

Keywords **–** Decoy Flare, Detection, Singular Value Decomposition, SVD, Tracking

1. Introduction:

Aerial infrared tracking plays an important role in military aerial reconnaissance, counter air-defense, and terminal guidance for many weapon systems such as air-to-air or surface-to-air missiles. In military applications, Infrared (IR) imaging has many merits including its ability against anti-interference, all-weather observations, high-guidance accuracy, and long range detection [1]. However, on the other hand, IR imaging has low-spatial resolution, low signal-to-noise (SNR) ratios, and lack of structural information [2]. Therefore, tracking aerial targets such as fighter aircraft is still challenging in presence of infrared jamming [3,4]. Research in this field is still ongoing and many IR tracking algorithms have been developed including for example Least Soft-threshold Squares Tracking (LSST) [5], Tracking-Learning Detection (TLD) [6], High speed tracking with kernelized Correlation Filters (KCF) [7], Long-term Correlation Tracking (LCT) [8], Continuous-Convolution Operators for Tracking C-COT [9], and Efficient Convolution Operators for Tracking (ECO) [10]. In addition, several algorithms have been developed for dim or small target tracking and detection in noisy background including Template Matching Tracking (TMT) [11, 12], Mean Shift (MS) [12, 14], Temporal Spatial Fusion Filtering (TSFF) [15], and Particle Filter (PF) [16, 17]. However, relying on the characteristics and properties of Singular Value Decomposition (SVD) that could potentially be utilized in IR tracking as will be shown later, there could be an opportunity for further development in this field. Thus, the focus in this research will be on developing an effective algorithm based on Singular Value Decomposition (SVD) that could automatically tracks aerial targets (fighter aircraft and helicopters) rapidly and accurately in the presence of infrared decoy flares based on infrared image sequence. SVD is a factorization of real or complex matrix M into three independent matrices in the form $M = U\Sigma V^T$. A two dimensions $N \times M$ matrix can be represented by its SVD as

$$[X]^N_M = {}_M[U]^M [S]^N_M [V]^N_N{}^T$$

$$U = [u_1, u_2, \ldots u_m], \qquad V = [v_1, v_2, \ldots v_n],$$

$$S = \begin{bmatrix} \sigma_1 & & & \\ & \sigma_2 & & \\ & & O & \\ & & & \sigma_n \end{bmatrix}$$

Where U and V matrices represent left and right singular vectors respectively, and Σ is diagonal matrix whose diagonal elements are the singular values.

Decoy flares are an aerial infrared countermeasure used by fighter aircraft and helicopters to decoy infrared guided missiles.

This paper organized as follows. Section 2 describes the procedure followed to conduct this work and the designed algorithms. Section 3 shows obtained results. Section 4 highlights the findings and provide an interpretation for the findings.

2. Methodology:

The goal in this work is to design one or more algorithms that can detect and track aerial targets in the presence of decoy flares. Manual features extraction and quantitative methods were used to segregate aerial targets from decoy flares.

This section organized as follows. Section 1 highlights the features of IR aerial targets. Section 2 states the assumptions relating to IR aerial targets and decoy flares. Section 3 explores SVD characteristics that can be used. Section 4 explains image's foreground subtraction technique used in this work. Finally, section 5 introduces proposed algorithms.

2.1. IR Aerial Target Features

An aircraft has an infrared-signature that is the visible representation of the exterior temperature of the aircraft fuselage [18]. Infrared-signature of an aircraft forms from several radiation-emitting sources including aircraft's metal skin, jet engine, and plume via air friction and hot exhausts [18]. Thus, infrared-signature usually has features that could allow the detection and tracking of aircraft. Figure (1) shows an example for an infrared image of a fighter aircraft and a helicopter. As shown in Figure (1), there are several features associated with aerial targets. These features including but not limited to: (1) brightness intensity, (2) dominant orientation, and (3) complexity.

(a)

(b)

Figure 1. Infrared image of (a) a fighter aircraft and (b) a helicopter

In addition, these features are also applicable to infrared-decoy flares as well. Figure (2) shows an example for an infrared image of decoy flares released from a helicopter. As shown in Figure (2), the above-mentioned features are also associated with decoy flares. However, the discrimination between aerial targets and flares relies on the distinguishable features. Therefore, several key assumptions are introduced in the following section.

Figure 2. Infrared-decoy flares discharged from a helicopter

2.2. Research key Assumptions

Table (1) comparatively shows the underlying assumptions relating to the features associated with aerial targets and infrared decoy flares. However, these features are impractical without the ability to measure them. Therefore, the following section highlight this topic.

Features	Aerial Target vs. DF[1]		
	FA[2]		H[5]
	A[3]	B[4]	
Brightness Intensity	A > DF	B < DF	H < DF
Dominant Orientation	A > DF	B > DF	H > DF
Complexity	A > DF	B > DF	H > DF

Table 1. Aerial target features vs. decoy flare features

(1) DF: Decoy Flare
(2) FA: Fighter Aircraft
(3) A: Fighter Aircraft with afterburner
(4) B: Fighter Aircraft without afterburner
(5) H: Helicopter

2.3. SVD Characteristics

SVD has several characteristics that are advantageous for measuring the features explained in the preceding section. Generally, these characteristics allowed SVD to be used in

several applications including oriented energy analysis, image energy truncation, and low rank approximation [19]. SVD singular value characteristics can be exploited to measure the brightness intensity and complexity of aerial targets. In addition, SVD singular vector characteristics can determine the dominate orientation of aerial targets. The use of SVD's characteristics for measuring aerial target features are explained in the following subsections.

2.3.1 Frobenius Based Brightness Intensity Measurement

In this section, an intuitive explanation of Frobenius norm based energy or brightness measurement concept is introduced. The image region of interest has to be classified as an aerial or a non-aerial target based on the gray-level intensity of image region. The assumption here is that, the aerial target corresponds to image region that has a gray-level intensity (brightness intensity) as described in Table (1). Based upon this concept and its performance in the presence of infrared decoy flares, an IR aerial target detection and tracking algorithm is then proposed.

Matrix norm is a scalar that reflects how large are the elements magnitude of the matrix [20, 21]. The Frobenius norm of $N \times M$ image region of interest (w_i) (where $i = 1, \dots, k$ and k is number of image regions per single frame) is defined as

$$Norm_F(w_i) = \sqrt{\sum_{i=1}^{m}\sum_{j=1}^{n} diag(A' * A)} = \sqrt{\sum_{i=1}^{m}\sum_{j=1}^{n} |A|^2}$$

Equivalently, Frobenius norm can be computed directly as follows

$$||w_i||_F = \sqrt{S_1^2 + \cdots + S_n^2} = \sqrt{\sum_{i=1}^{n} S_i^2} \ , i = 1, \dots, n$$

Where $S_1 \dots S_n$ are the singular values that result from the SVD of the matrix(w_i). Thus, Frobenius norm value can be used as metric to measure and compare aerial targets brightness intensity.

2.3.2 SVD Based Dominant Orientation Measurement

The aim of this section is to introduce the concept of dominant orientation of geometric structure in image region of interest. Here the image region corresponds to an object that has to classify as either an aerial or a non-aerial target. By using this concept, this implies classifying objects according to their orientation. Therefore, this approach is appropriate when the aerial target is assumed to be oriented as explained in Table (1). Based upon this concept and its performance in the presence of decoy flares, an IR target detection and tracking algorithm is then proposed.

The geometric structure can be estimated using image gradient i.e. differences among pixels. It is well known in image processing that the gradient of image is the directional change in the intensity as shown in Figure (3).

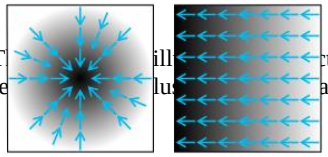

Figure 3. T ill tion of the gradie lu alues.

The gradient matrix of image region of interest depends on the method used to calculate the discrete derivatives. For example, consider an image arranged as matrix $A(x, y)$, then, the gradient of $N \times N$ image region w_i is defined as

$$G_{w_i} = \begin{bmatrix} . & . \\ . & . \\ . & . \\ A_x(k) & A_y(k) \\ . & . \\ . & . \\ . & . \end{bmatrix}, \ k \in w_i$$

Where $[A_x(k),\ A_y(k)]^T$ indicates the gradient of the image at point (x_k, y_k). The gradient G_{w_i} of $N \times N$ image region (w_i) in x and y directions is produced by first converting w_i to a column-stacked $1 \times N^2$ vector $\vec{\boldsymbol{n}}$ and then applying two-dimensional convolution with the filters [22]

$$\tfrac{1}{2} \times \begin{bmatrix} 0 & 0 & 0 \\ -1 & 0 & 1 \\ 0 & 0 & 0 \end{bmatrix} (in\ x\ direction),$$

$$\tfrac{1}{2} \times \begin{bmatrix} 0 & 0 & 0 \\ -1 & 0 & 1 \\ 0 & 0 & 0 \end{bmatrix} (in\ y\ direction)$$

Or the filters

$$\frac{1}{8} \times \begin{bmatrix} -1 & 0 & 1 \\ -2 & 0 & 2 \\ -1 & 0 & 1 \end{bmatrix} (in\ x\ direction),$$

$$\tfrac{1}{8} \times \begin{bmatrix} -1 & -2 & -1 \\ 0 & 0 & 1 \\ 1 & 2 & 1 \end{bmatrix} (in\ y\ direction)$$

The gradient matrix G_{w_i} of w_i is then obtained by horizontally combining the arrays derived from the 2-D convolution of above-mentioned filters with $\vec{\boldsymbol{n}}$.

The dominant orientation of w_i is obtained by applying the economic form of singular value decomposition (SVD) of G_{w_i} [23] [24] as follows

$$G_{w_i} = USV^T = U \begin{bmatrix} S_1 & 0 \\ 0 & S_2 \end{bmatrix} [v_1 \quad v_2]^T$$

Where U and V are orthonormal matrices and they respectively represent the left and right singular vectors, S_1 and S_2 represent the singular values. The column vector $\boldsymbol{v}_1$ represents the dominant orientation of gradient field of image region of interest G_{w_i} . On the other hand, $\boldsymbol{v_2}$ represents the dominant edge orientation. Certainty of the dominant orientation estimate could be measured by obtaining the difference ΔS between S_1 and S_2 [25]. Thus, the accuracy of dominance could be calculated as

$$\Delta S = S_1 - S_2$$

Alternatively, the difference normalized is defined as

$$\Delta S = \frac{S_1 - S_2}{S_1} \times 100$$

The direction of dominant orientation is the angle Θ between $\boldsymbol{v}_1$ and the horizontal axis such that

$$\Theta = \tan^{-1} \frac{y}{x}$$

Where y and x are the $\boldsymbol{v}_1$ components.

This explanation of local dominant orientation is validated experimentally as shown in figure (4).

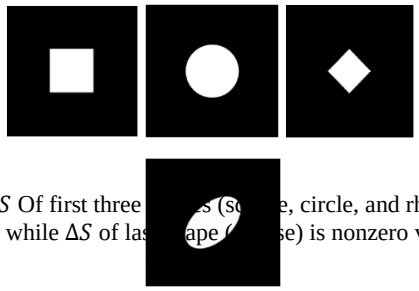

Figure 4. ΔS Of first three s (s e, circle, and rhombus) are zero, while ΔS of las ape (se) is nonzero value.

2.3.3 Low Rank Based Complexity Measurement

Low rank based complexity measure using singular value decomposition (SVD) presented in this section. Complexity determined by the number of signaler values that are required for low rank approximation. SVD can offer low rank approximation by considering only non-zero singular values [2]. This is useful to measure the complexity of image region of interest such that, the smaller the difference between the rank of original image region and the approximated image, the more complex is the image region. The w_i can be expressed as the sum of rank-one matrices [2] as follows

$$w_i = \sum_{j=1}^{k} S_j U_j V_j^T = S_1 U_1 V_1^T + S_2 U_2 V_2^T + \cdots + S_k U_k V_k^T$$

Where k is the rank of w_i. The partial sum captures as much of "energy" contained in w_i. An intuitive approach to estimate complexity is as follows

$$\textit{Complexity} = \frac{\textit{Number of zero value singular values}}{\textit{Total number of singular values}}$$

Figure (5) shows the singular values of a grayscale image. As can be seen in this figure, some singular values are equal to zero or are very small. The number of these small singular values varies from one image to another depending on the details of the image.

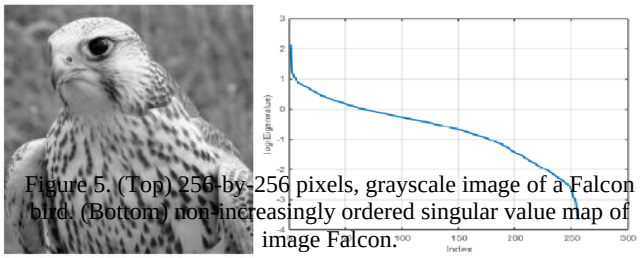

Figure 5. (Top) 256-by-256 pixels, grayscale image of a Falcon bird. (Bottom) non-increasingly ordered singular value map of image Falcon.

2.4. Foreground Subtraction

Foreground subtraction is necessary to allow image's foreground to be extracted for detection, tracking, and further processing. The method used to extract image's foreground in this work is based on threshold detection. If the input pixel is above the threshold, then that pixel will be equal to one, and zero otherwise. The 170 value was selected as a threshold as long it captures the overall details of the target without including unnecessary background noise or sacrificing target details. Figure (6) highlights this issue.

y ima luced by threshold detection (with original image (bottom)

2.5. Proposed Algorithms

Three algorithms are introduced in this section. These algorithms were developed tacking into account SVD singular values and vectors characteristics that can be exploited for detecting and tracking aerial targets in the event of releasing decoy flares. Each algorithm detects and tracks aerial targets using only one of aerial target features. Pseudo codes of these algorithms explained in the following subsections.

2.3.4 Frobenius Based Brightness Intensity Algorithm

Read video frame
While continue to read and display video frames until no more frames are available to read
Convert RGB image to grayscale image
Perform foreground subtraction (turn grayscale image to binary image to allow an image's foreground to be extracted for further processing)
Find connected components in binary image (set of pixels that form a connected group)
Find centroid, position and size of smallest containing box for each connected component
For each connected component
Extract corresponding sub-matrix
Calculate Frobenius Norm of sub-matrix
Save calculated Frobenius Norm
Return max Frobenius Norm
Return centroid and bounding box of connected component that has max Frobenius Norm
Insert x-coordinate in video frame
Insert y-coordinate in video frame
Insert value of max Frobenius Norm in video frame
Display processed video frame
Pause temporarily (time depends on the original frame rate speed) to see all frames

2.3.5 SVD Based Dominant Orientation Algorithm

Read video frame
While continue to read and display video frames until no more frames are available to read
Convert RGB image to grayscale image
Perform foreground subtraction (turn grayscale image to binary image to allow an image's foreground to be extracted for further processing)
Find connected components in binary image (set of pixels that form a connected group)
Find centroid, position and size of smallest containing box for each connected component
For each connected component
Extract corresponding sub-matrix
Calculate gradient in x and y direction
Calculate SVD of gradient
Calculate difference ΔS between S_1 and S_2
Save value of ΔS
Return max ΔS
Return centroid and bounding box of connected component that has max ΔS
Insert x-coordinate in video frame
Insert y-coordinate in video frame
Insert value of max ΔS in video frame
Display processed video frame
Pause temporarily (time depends on the original frame rate speed) to see all frames

2.3.6 Low Rank Based Complexity Algorithm

Read video frame
While continue to read and display video frames until no more frames are available to read
Convert RGB image to grayscale image
Perform foreground subtraction (turn grayscale image to binary image to allow an image's foreground to be extracted for further processing)
Find connected components in binary image (set of pixels that form a connected group)
Find centroid, position and size of smallest containing box for each connected component
For each connected component
Extract corresponding sub-matrix
Calculate SVD of sub-matrix
Calculate complexity (C) = Number of zero singular values / Total number of singular values
Save value of C
Return max C
Return centroid and bounding box of connected component that has max C
Insert x-coordinate in video frame
Insert y-coordinate in video frame
Insert value of max C in video frame
Display processed video frame
Pause temporarily (time depends on the original frame rate speed) to see all frames

3. Results

The purpose of this research is to design an algorithm capable of detecting and tracking aerial targets in the presence of decoy flares. Therefore, the three algorithms defined in the preceding section have been tested in the presence of decoy flares. The results of two types of aerial targets are shown in following subsections.

3.1. Helicopters

Table (2) as well Figures (7-10), show the performance of the three algorithms. Table (3) shows the results.

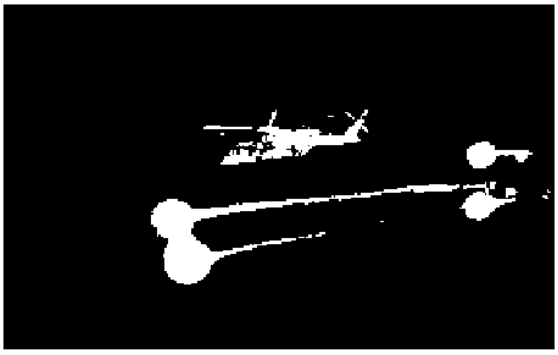

Figure 7. Binary image of Helicopter & decoy flares

Figure 8. Orientation based discrimination (max)

Figure 9. Brightness based discrimination (min)

Figure 10. Complexity based discrimination (max)

Object	Orientation (ΔS)	Brightness ($Frobenius\ Norm$)	Complexity (C)
1	54.9514	37.2424	0.9811
2	73.9111	5.7446	0.6667
3	52.2408	1.4142	0.5000
4	33.0036	25.6515	0.9655
5	66.6667	1.0000	0.5000
6	51.3973	3.7417	0.7500
7	52.2408	1.4142	0.5000
8	15.9208	2.8284	0.7500
9	10.1371	3.1623	0.7500
10	66.6667	1.0000	0.5000
11	36.7544	1.7321	0.6667
12	57.0094	1.7321	0.5000
13	66.6667	1.0000	0.5000
14	29.2893	2.2361	0.6667
15	58.5961	2.4495	0.6667
16	57.0094	1.7321	0.5000
17	59.8453	2.6458	0.7500
18	66.6667	1.0000	0.5000
19	43.6710	2.4495	0.7500
20	52.2408	1.4142	0.5000
21	29.7906	16.4317	0.9524
22	39.4829	15.1327	0.9333
23	44.7601	3.0000	0.7500
24	8.3635	4.7958	0.8333
25	35.6429	2.0000	0.6667
26	4.6537	1.7321	0.6667

Table 2. Performance of the three algorithms

Algorithm	Performance
Brightness based discrimination	Excellent
Orientation based discrimination	Acceptable
Complexity based discrimination	Poor

Table 3. Results of the three algorithms

3.2. Fighter Aircraft

Table (4) and Table (5) as well Figures (11-17), show the performance of the three algorithms for fighter aircraft with and without afterburner. Table (6) shows the results.

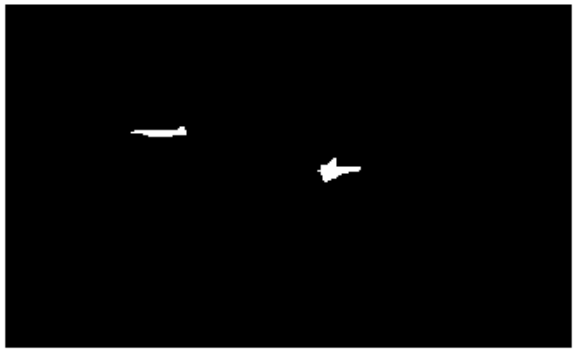

Figure 11. Binary image of fighter aircraft and decoy flares

Figure 12. Orientation based discrimination (max)

Figure 13. Brightness based discrimination (max)

Figure 14. Complexity based discrimination (min)

Object	Orientation (ΔS)	Brightness ($Frobenius\ Norm$)	Complexity (C)
1	61.9857	9.6437	0.8571
2	36.3000	10.3923	0.9286

Table 4. Performance of the three algorithms (without Afterburner)

Algorithm	Performance
Brightness based discrimination	Excellent
Orientation based discrimination	Poor
Complexity based discrimination	Poor

Table 5. Results of the three algorithms

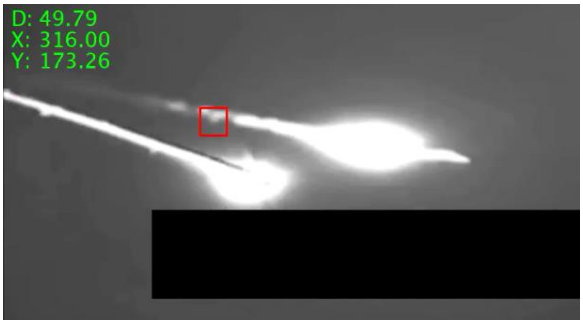

Figure 15. Orientation based discrimination (max)

Figure 16. Brightness based discrimination (max)

https://dx.doi.org/10.29322/IJSRP.13.09.2023.p14111

Figure 17. Complexity based discrimination (max)

Object	Orientation (ΔS)	Brightness ($Frobenius\ Norm$)	Complexity (C)
1	49.79	121.82	0.88

Table 6. Performance of the three algorithms (with Afterburner)

4. Discussion

The interpretation and significance of the findings in the results are explained in this section. Brightness based discrimination proved to be effective against decoy flares for both aerial targets (fighter aircraft & helicopters) since this feature is distinguishable. For helicopters, the results show that they emit smaller infrared radiation compared to decoy flares. For fighter aircraft, the emitted IR radiation is greater than the radiation of decoy flares if afterburner is used. However, in the case of no afterburner is used, decoy flares usually emit more or equal IR radiation compared to the fighter aircraft. Figure (12) and Figure (13) show the IR radiation emitted by decoy flares compared to aircraft. In this situation, the algorithm should be adjusted to track minimum brightness.

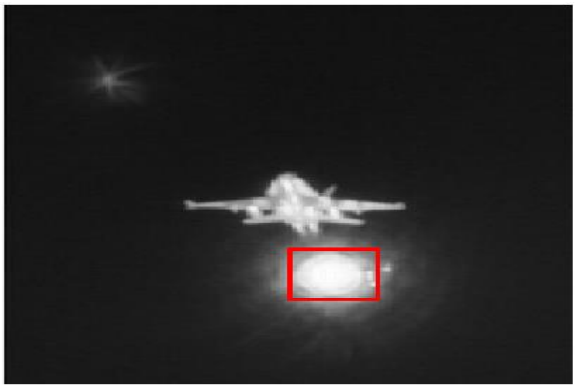

Figure 18. IR radiation emitted by decoy flares compared to aircraft

Figure 19. IR radiation emitted by decoy flares compared to aircraft

Orientation based discrimination showed poor performance in tracking fighter aircraft with and without afterburner. The tracking was always toward the extended part of the plume generated by the exhaust as shown in Figure (13). However, orientation based discrimination with helicopters showed acceptable performance mainly due to the orientation of rotor blades. The length and width of rotor blades generate maximum orientation as shown in Figure (1) and Figure (2).

Figure 20. Orientation based discrimination follow the extended plume generated by the exhaust

Complexity based discrimination showed poor and unstable performance in all cases. Figure (14) shows the performance in tracking supersonic aerial target.

Figure 21. Performance of complexity based algorithm in detecting and tracking supersonic target

5. Conclusion

In summary, the goal of this research is to design an algorithm capable of detecting and tracking aerial targets (fighter aircraft and helicopters) in the presence of decoy flares. Features including brightness intensity, dominant orientation and complexity were used for the discrimination against decoy flares. SVD characteristics including oriented energy analysis, image energy truncation, and low rank approximation were used to measure these features. Obtained results showed that brightness based discrimination has a better performance against decoy flares compared to orientation based/complexity based discrimination. In addition, orientation based discrimination well performed with helicopters due to the dimensions of their rotor blades.

References

[8] C. Ma, X. Yang, C. Zhang, and M.-H. Yang, “Long-term correlation tracking,” in Proceedings of the IEEE Conference on Computer Vision and Pattern Recognition, CVPR ’15, pp. 5388–5396, 2015.

[5] D.Wang, H. Lu, andM.-H. Yang, “Least soft-threshold squares tracking,” in Proceedings of the 26th IEEE Conference on Computer Vision and Pattern Recognition (CVPR ’13), pp. 2371–2378, June 2013.

[12] E. Lee, H. Yoo, E. Gu, et al., Moving dim-target tracking algorithm using template matching, in: International Conference on Technological Advances in Electrical, Electronics and Computer Engineering, 2013, pp. 294–297.

[18] Elsaidy, Amir & Kassem, Mohamed & Tantawy, Hesham & Elbasuney, Sherif. (2017). The Infrared Spectra of Customized Magnesium/Teflon/Viton (MTV) Decoy Flares to Thermal Signature of Jet Engine. Journal of Engineering Science and Military Technologies. 17. 1-12. 10.21608/ejmtc.2017.21267.

[16] F. Wang, E. Liu, J. Yang, S. Yu, et al.,Target tracking in infrared imagery using a novel particle filter, Chin. Opt. Lett. 7 (7) (2009) 576–579.

[3] Hu, Yangguang & Xiao, Mingqing & Zhang, Kai & Wang, Xiaotian. (2019). Aerial Infrared Target Tracking in Complex Background Based on Combined Tracking and Detecting. Mathematical Problems in Engineering. 2019. 1-17. 10.1155/2019/2419579.

[2] H. Xin and S. Tang, “Target detection and tracking in forward looking infrared image sequences using multi morphological filters,” in Proceedings of the International Symposium on Image & Signal Processing & Analysis, 2007.

[14] I. Leichter, Mean shift trackers with cross-bin metrics, IEEE Trans. Pattern Anal. Mach. Intell. 34 (4) (2012) 695–706.

[25] J. Bigun, G. H. Granlund, and J. Wiklund, Multidimensional orientation estimation with applications to txture analysis and optical flow, IEEE Transactions on Pattern Analysis and Machine Intelligence 13(8) (1991), 775–790.

[24] J. Bigun, G. H. Granlund, and J. Wiklund, “Multidimensional orientation estimation with applications to texture analysis and optical flow,”IEEE Trans. Pattern Anal. Mach. Intell., vol. 13, no. 8, pp. 775–790, Aug. 1991.

[7] J. F. Henriques, R. Caseiro, P. Martins, and J. Batista, “High Speed tracking with kernelized correlation filters,” IEEE Transactions on Pattern Analysis andMachine Intelligence, vol. 37, no. 3, pp. 583–596, 2015.

[4] Kun, Qian & Zhou, Hui-Xin & Rong, Shenghui & Wang, Bingjian & Cheng, Kuanhong. (2017). Infrared dim-small target tracking via singular value decomposition and improved Kernelized correlation filter. Infrared Physics & Technology. 82. 10.1016/j.infrared.2017.02.002.

[21] Kuo-Liang Chung, C. Shen, L. Chang, "A novel SVD- and VQ-based image hiding scheme", Pattern Recognition Letters, 2002, 1051-1058

[17] L. Chang, Z.H. Liu, S.T. Wu, Tracking of infrared radiation dim target based on mean-shift and particle filter, Guidance, Navigation and Control Conference (CGNCC), IEEE Chinese, 2014, pp. 671–675.

[9] M. Danelljan, A. Robinson, F. S. Khan, and M. Felsberg, “Beyond correlation filters: learning continuous convolution operators for visual tracking,” in Proceedings of the European Conference on Computer Vision, pp. 472–488, 2016.

[10] M. Danelljan, G. Bhat, F. S. Khan, and M. Felsberg, “ECO: efficient convolution operators for tracking,” in Proceedings of the 30th IEEE Conference on Computer Vision and Pattern Recognition, CVPR ’17, pp. 6931–6939, 2017.

[20] R. Liu and T. Tan, “A SVD-Based Watermarking Scheme for Protecting Rightful Ownership,” IEEE Transaction on Multimedia, 4(1), pp.121-128, March 2002

[11] R.M. Liu, Y.H. Lu, C.L. Gong, et al., Infrared point target detection with improved template matching, Infrared Phys. Technol. 55 (4) (2012) 380–387.

[19] Sadek, Rowayda. (2012). SVD Based Image Processing Applications: State of The Art, Contributions and Research Challenges. International Journal of Advanced Computer Science and Applications - IJACSA. 3. 10.14569/IJACSA.2012.030703.

[15] W.H. Wang, Z.D. Niu, Z.P. Chen, Temporal-spatial fusion filtering algorithm for small infrared moving target detection, Infrared Laser Eng. 34 (6) (2005) 714–718.

[23] X. Feng and P. Milanfar, "Multiscale principal components analysis for image local orientation estimation," in Proc. 36th Asilomar Conf. Signals, Syst. Comput., Pacific Grove, CA, Nov. 2002, vol. 1, pp. 478–482.

[1] Y. Li, S. Liang, B. Bai, and D. Feng, "Detecting and tracking dim small targets in infrared image sequences under complex backgrounds," Multimedia Tools and Applications, vol. 71, no. 3, pp. 1179–1199, 2014.

[22] Zhu, Xiang & Milanfar, Peyman. (2010). Automatic Parameter Selection for Denoising Algorithms Using a No-Reference Measure of Image Content. IEEE transactions on image processing: a publication of the IEEE Signal Processing Society. 19. 3116-32. 10.1109/TIP.2010.2052820.

[6] Z. Kalal, K. Mikolajczyk, and J. Matas, "Tracking-learning detection," IEEE Transactions on Pattern Analysis and Machine Intelligence, vol. 34, no. 7, pp. 1409–1422, 2012.

[13] Z.L. Wang, Q.Y. Hou, L. Hao, Improved infrared target-tracking algorithm based on mean shift, Appl. Opt. 51 (21) (2015) 5051–5059.

AUTHORS

First Author – Bader Algahtani, PhD student, Electronic and communication engineering, King Abdulaziz University.

Baderm2000@hotmail.com

Second Author – Prof. Adnan Affandi, Electronic and communication engineering, King Abdulaziz University.

adnanaffandi@yahoo.co.uk